Appl. Phys. A 69 [Suppl.], S841–S844 (1999) / Digital Object Identifier (DOI) 10.1007/s003399900314

Applied Physics A
Materials
Science & Processing

Structure formation in excimer laser ablation of stretched poly(ethylene therephthalate) (PET): the influence of scanning ablation

F. Wagner, P. Hoffmann*

Institute of Applied Optics, Swiss Federal Institute of Technology, Micro Engineering Department, CH-1015 Lausanne, Switzerland
(Fax: +41-21/693-37-01, E-mail: Patrik.Hoffmann@epfl.ch)

Received: 21 July 1999/Accepted: 1 September 1999/Published online: 28 December 1999

Abstract. Multiple pulse laser ablation of stretched PET is performed with an ArF excimer laser (193 nm) in order to produce micro channels. The surface structure remaining after "scanning ablation", in which the sample is moved during irradiation, is compared to the known results upon "static ablation".

We observed that the debris contribution is enhanced upon scanning ablation, which has a major impact for the channels used in micro-fluidic applications. A more fundamental change of the channel floor structure, as seen by SEM, occurs at high fluences and short mask lengths. The channel floor structure originates from the structure on the irradiated ramp at the end of the channel. The "scanning structure" appears only if the irradiated end ramp forms an angle higher than $10.55(\pm 0.15)^\circ$ with the non-irradiated sample surface. The angle of light incidence is not responsible for the structure changes, in agreement with literature reports. Other possible mechanisms are briefly discussed.

PACS: 42-62; 81-65; 81-05

Excimer lasers are now established for a wide variety of applications. However, basic investigations are still necessary for a better understanding of the involved processes. In applications of excimer laser ablation, the substrates are often scanned under the beam in order to produce structures that are larger than the illuminated area. This, for example, is one of the easiest ways to produce micro-channels of highly variable geometry in plastic substrates for lab-on-a-chip applications. As Roberts and co-workers [1] have already observed, the wettability changes drastically when going from "static ablation" (without scanning during irradiation) to scanning ablation. Therefore it is important to study in detail the differences induced by "scanning ablation".

This paper deals mainly with the differences in surface topography between static and scanning ablation of stretched PET films. In summary, three types of structures can be distinguished. At fluences below the ablation threshold, LIPS (light-induced periodic structure) [2] can be observed. At fluences around the ablation threshold, dendrite-like structures develop if the irradiation is carried out in vacuum [3, 4]. At fluences well above the ablation threshold, a nap or wall-type structure develops in stretched PET foils [5–7].

We are working in this last fluence range, where the structures observed after static irradiation [8] get more pronounced with increasing number of pulses and increasing fluence. This was investigated in detail by [9]. We will refer to this nap or wall-type structure as "static structure".

1 Experimental

For all experiments, commercial stretched poly(ethylene terephthalate) (PET) films with a thickness of 100 μm were used (Melinex, type S, ICI, GB). The samples were usually exposed to 200 pulses of an ArF excimer laser at 193 nm (LPX 205, Lambda Physik, D) in air. The investigated fluences ranged from 75 to 1200 mJ/cm^2, i.e. well above the measured ablation threshold of 36 mJ/cm^2. The repetition rate of the pulses varied between 1 and 50 Hz. In the experimental setup, we used a beam homogenizer (Excitech, GB) in order to illuminate a rectangular mask that was imaged by an objective (Exitech, GB) with a 10-fold size reduction on the sample. For the channel production, the sample was mounted on a high precision stepper motor driven translation stage (Microcontrole, F). The minimum step size of the translation stage (0.1 μm) was well below the optical resolution (≈ 3 μm) of the setup. The structure of the ablated surfaces was investigated by field emission secondary electron microscopy (FESEM) (Philips XL 30 FE, D) at 1 kV acceleration voltage, without any conductive coating on the sample.

To produce channels longer than the maximally illuminated area, two ablation "modes" were studied:

1. The "static ablation" mode, where we used a rectangular mask of 0.4×10 mm^2 to drill a hole of 40 μm in width

*Corresponding author.

COLA'99 – 5th International Conference on Laser Ablation, July 19–23, 1999 in Göttingen, Germany

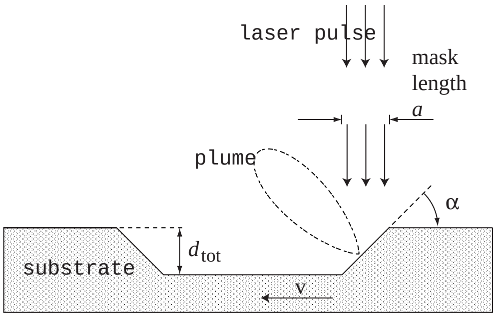

Fig. 1. Schematic presentation of channel preparation by scanning ablation. The sketch shows the channel in a cross-section along the channel direction. The left-hand side corresponds to the beginning of the channel and the right-hand side to its end

and 1000 μm in length. The sample was then moved by 1000 μm along the longer axis and the next hole was drilled in contact with the first one, and so on.

2. The "scanning mode", where we also used a rectangular mask to illuminate an area of 40 μm times the effective mask length a (Fig. 1), but simultaneously moving the sample in the direction of a during the illumination.

In both modes, the channel depth $d_{tot} = n \times h(\Phi)$ (Fig. 1) depends on the number of pulses n (per surface area) and the ablation rate per pulse $h(\Phi)$ at fluence Φ. In scanning ablation n is given by $n = \nu a/v$, where ν is the pulse repetition rate of the laser, v the scanning velocity of the sample, and a the effective mask length. Usually we used $n = 200$, which results at $1200\,\mathrm{mJ/cm^2}$ in channels having a transverse cross-section of about $40 \times 40\,\mu\mathrm{m}^2$.

2 Channel geometry and scanning ablation parameters

In scanning ablation with more than one pulse per mask length the irradiated area theoretically has the shape of a stairway. The step width s is given by $s = v/\nu$ and the step height is defined by the ablation rate per pulse $h(\Phi)$. If, as in our case, the step width s is below the optical resolution of the setup, the stairway simply becomes a ramp. Its angle α is given by $\tan(\alpha) = d_{tot}/a$. As the sample is moved further, a flat channel forms between the ramp at the beginning of the channel and the irradiated one at the end (Fig. 1).

3 Results

3.1 Debris contribution to the structure

The important difference in wettability of micro-channels produced by scanning and static ablation [1] is strongly influenced by the different amount of redeposited debris in the channel. In static ablation, each laser shot impinges on the same position as the previous one, removing the already redeposited debris. Debris can therefore accumulate close to the channel, but not inside.

In scanning ablation, however, every point of the channel floor is near the irradiated surface at some point. As a consequence, an accumulation of the debris also occurs in the channel. Additionally, when using high fluences and short mask lengths, i.e. having large ramp angles α, a kind of "self-PLD" (PLD: pulsed laser deposition) occurs in the channel. In this case, the tilt of the irradiated surface with respect to the channel floor (Fig. 1) has the same effect as approaching the substrate (channel floor) and target (irradiated end ramp) in a PLD experiment: it increases the deposition rate of target material on the substrate (Fig. 2).

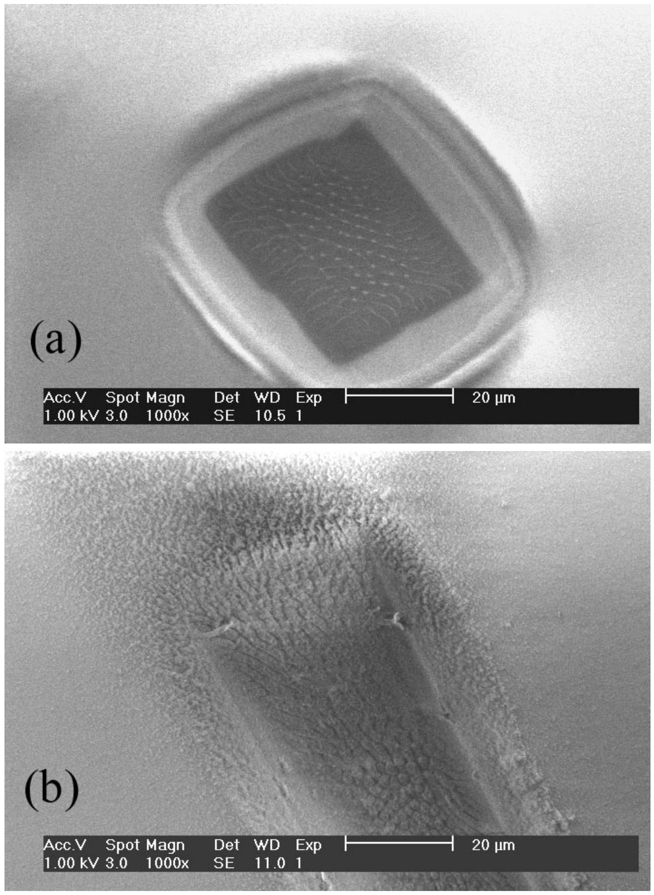

Fig. 2a,b. FESEM micrographs of **a** statically ablated structure and **b** the beginning of a channel produced by scanning ablation. A strong debris contribution due to "self-PLD" is visible in **b**. (Parameters: $\Phi = 600\,\mathrm{mJ/cm^2}$, $n = 200$, $a = 50\,\mu\mathrm{m}$, **b** $\alpha = 32°$)

After scanning ablation, the surface chemistry of the channel floor is therefore determined by the hydrophilic debris and no longer by the hydrophobic polymer. Chemical analyses of the channel floor obtained by scanning ablation are under investigation and will be compared with the published results of extensive studies from static ablation [10]. As α increases the debris covers more and more the basic surface structure, which is described below.

3.2 The structure on the channel floor

In static ablation as well as in scanning ablation with long masks and low fluences, we observed the well-known structure on the channel floor [7, 9] (Fig. 3a). It is indicated by "O" in Table 1 and will be referred to as "static structure". The formation of this structure can be attributed to the frozen stresses in the material, which are caused by the fabrication process [8]. As a result, the main orientation of the struc-

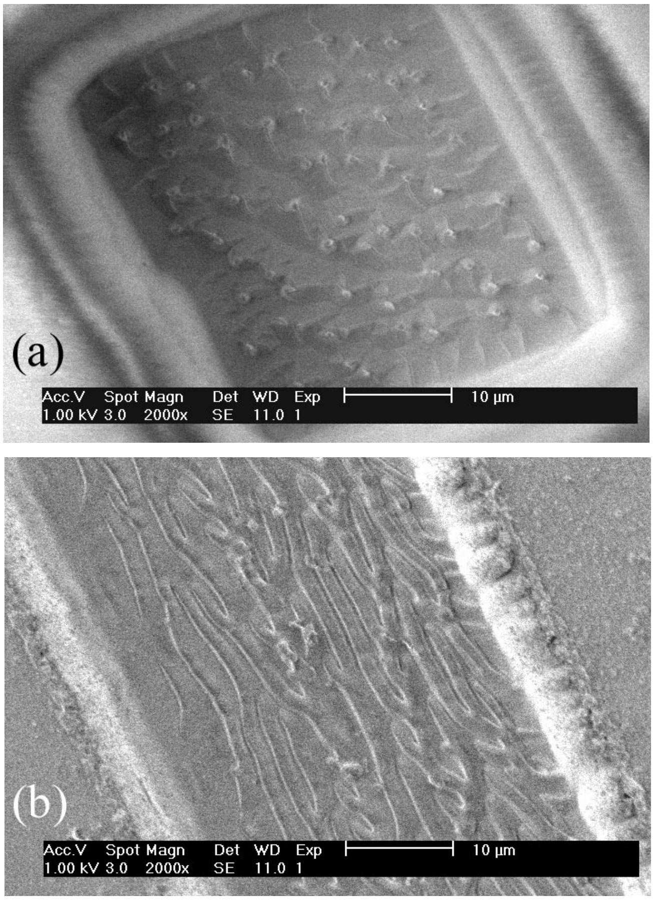

Fig. 3a,b. FESEM micrographs of the channel floor of two samples produced with the same fluence (150 mJ/cm^2) and the same number of pulses ($n = 200$). **a** static ablation results in the "static structure". **b** Scanning ablation with $a = 50$ µm results in the new "scanning structure"

Table 1. Parameter range where the "scanning structure" (X) and the "static structure" (O) were observed ($n = 200$ for all samples)

Φ (mJ/cm^2)	a (µm)			
	50	100	200	1000
75	O	O	O	O
150	X	O	O	O
300	X	X	O	O
600	X	X	O	O
1200	X	X	X	O

ture is given in uniaxially stretched samples by the orientation of the stress and not by the direction of the channel. In biaxially stretched samples, a nap-type structure [8] (Fig. 3a) develops.

Only when carrying out scanning ablation with high fluences and/or short mask lengths did the new structure (Fig. 3b) show up. It is indicated by "X" in Table 1 and will be referred to as "scanning structure". It is characterized by flow-like stripes having about the same period as the static structure (2–3 µm). The fact that the principal orientation of these stripes is given in all samples by the direction of the channel indicates that the frozen stresses do not play an important role in the scanning structure formation.

Varying the repetition rate ν in the range 1–50 Hz for both static and scanning structures showed only a negligible influence on structure formation on our 100 µm thick samples. The scanning velocities applied in our experiments ($\upsilon <$ 250 µm/s) are negligible compared with the velocities of the ejected particles at the applied fluences (0.2–10 km/s [11, 12]). Therefore the influence of the scanning velocity on structure change can be excluded. This was confirmed by an experiment in which the scanning structure was obtained without scanning the sample [13].

4 Discussion

The observed structure change on the channel floor originates from the processes occurring on the irradiated end ramp of the channel. The structure on the end ramp and the structure on the channel floor are always very similar. The only exception is that the ramps can become completely smooth, whereas we never observed a smooth channel floor [13]. By measuring the ramp angles α with an profilometer (Alpha-Step 200, Tencor Instruments) we found that all samples exhibiting the scanning structure on the channel floor had ramp angles higher than 10.7°. All samples showing the static structure had ramp angles lower than 10.4°. We can thus define a limiting ramp angle $\alpha_l = 10.55(\pm 0.15)°$ where the structure change occurs.

Hopp et al. [9] investigated static ablation on inclined substrates. Comparing our results with their work, it is clear that the system can no longer be described only by the surface, the surrounding gas, and the light. As a matter of fact, they did not observe any significant changes of surface structure up to an angle of 60° between the normal to the irradiated area and the incident light. The only difference between static ablation on an inclined substrate and scanning ablation is that in scanning ablation the irradiated area is inclined, not only with respect to the incident light, but also with respect to the rest of the sample. Consequently, a theory which can possibly explain the structure change has to include the geometrical environment of the irradiated area.

However, up to now it is not clear how the geometrical environment could influence the structure formation. Shock wave influences originating from either the shock wave in the atmosphere or from the shock wave in the substrate itself, as well as a possible difference in surface tension occurring in the liquid layer should be considered. None of these hypotheses is proven yet. But it seems obvious that a lateral temperature gradient, eventually affecting the surface tension, which might be present on the ramp at $\nu = 50$ Hz, is not important for the structure change because the structure also changed in the control experiment at low repetition rate ($\nu = 1$ Hz).

5 Conclusion

We compared the structures produced by scanning ablation of stretched PET with the results of static ablation.

It was shown that the debris redeposition is much more important in scanning ablation than in static ablation, resulting in a radical change of wettability. Two main causes are identified: (1) no cleaning of the channel floor by subsequent laser pulses and (2) "self-PLD" process.

Another difference between static and scanning ablation is the presence of more than one structure in the case of scanning ablation. The structure which will be observed after scanning ablation depends on the ramp angle during the fabrication of the channel. A new surface structure named "scanning structure" appears if the ramp angle α exceeds 10.55°. There is no influence of the pulse repetition rate ν and scanning velocity v on the structure change from static to scanning structure.

When comparing the results of scanning ablation with the results of static ablation on inclined substrates we see that the geometrical arrangement of the sample near the ablated region seems to influence the structure formation. However, up to now it is not clear whether the ramp angle is really the determining parameter and how the environment can influence the structure formation.

References

1. M.A. Roberts, J.S. Rossier, P. Bercier et al.: Anal. Chem. **69**, 2035 (1997)
2. M. Csete, Z. Bor: Appl. Surf. Sci. **133**, 5 (1998)
3. J. Heitz, E. Arenholz, D. Bäuerle et al.: Appl. Phys. A **56**, 329 (1993)
4. J. Heitz, E. Arenholz, D. Bäuerle et al.: Appl. Surf. Sci. **81**, 103 (1994)
5. R. Srinivasan, V. Mayne-Banton: Appl. Phys. Lett. **41**, 576 (1982)
6. L. Wefers, D. Bosbach, W. Rammensee et al.: Appl. Surf. Sci. **69**, 418 (1992)
7. T. Bahners, W. Kesting, E. Schollmeyer: Appl. Surf. Sci. **69**, 12 (1993)
8. E. Arenholz, V. Svorcik, T. Kefer et al.: Appl. Phys. A **53**, 330 (1991)
9. B. Hopp, M. Csete, K. Révész et al.: Appl. Surf. Sci. **96**-**98**, 611 (1996)
10. S. Lazare, R. Srinivasan: J. Phys. Chem. **90**, 2124 (1986)
11. R. Kelly, A. Miotello, B. Braren et al.: Appl. Phys. Lett. **60**, 2980 (1992)
12. P.E. Dyer, J. Sidhu: J. Appl. Phys. **64**, 4657 (1988)
13. F. Wagner, P. Hoffmann: Appl. Surf. Sci. (accepted)